Photonic-Assisted Microwave Frequency Measurement With Adjustable Channel Bandwidth Based on Spectrum-Controlled Brillouin Phase Shift

Di Wang, Xindong Zhang, Shuang Liu, Zhangyi Yang, Cong Du, Jiaqi Li, *Member, IEEE*, and Wei Dong

***Abstract*—A photonics-based channel bandwidth tunable microwave frequency measurement (MFM) is analyzed and verified, which is implemented based on the principle of the frequency-to-phase-slope mapping (FTPSM) in stimulated Brillouin scattering (SBS). The spectrum-controlled Brillouin phase shift curve is created by using an optical frequency comb (OFC) pump instead of a single pump. As a result, the Brillouin phase shift response is superimposed to further realize a flexible and adjustable measurement bandwidth. Meanwhile, thanks to the relationship between the OFC pump and the unknown signal, the frequency measurement can be achieved by the property of monotonous frequency-to-phase-slope mapping. A proof-of-concept experiment is performed to verify the feasibility of the approach. By changing the number of OFC lines, the channel bandwidths of 500, 700, or 900 MHz are demonstrated, with a measurement error lower than 35 MHz. We believe that this FTPSM-based MFM system is a promising solution for radio frequency (RF) channelized receiver.**

***Index Terms*—Microwave photonics, stimulated brillouin scattering, frequency measurement, frequency-to-phase-slope mapping.**

I. Introduction

With the increasing requirements for the transmission bandwidth of radio frequency (RF) signal and the gradually complex electromagnetic environment, frequency identification technology in light of large frequency range and high accuracy has demonstrated potential applications in many fields, such as electronic warfare systems, modern radar, and wireless communication [1]. Compared with electrical-assisted frequency identification, the photonics-assisted frequency identification strategy is discussed more widely due to its excellent advantages of wide bandwidth and immunity to electromagnetic interference [2], [3].

In recent decades, various methods of microwave frequency measurement have been consecutively proposed, including the frequency-to-power mapping [4]–[8], which has been commonly used to convert frequency into amplitude. It is achieved by comparing the response functions of different channels, thus obtaining a monotonous response function, also known as the amplitude comparison function (ACF). However, this approach may be limited due to the trade-off between the frequency range and the accuracy. To achieve a balance between them, we can adjust or replace the dispersion element (DE), such as laser wavelengths [4], polarization state [5], pilot tones [6], and different types of modulators [7], [8]. In addition, the mapping of frequency to time and frequency to voltage can be realized by accurately controlling the SBS-based optical filter and adjusting the time-delay value of two loops [9], [10]. Unfortunately, the measurement error is relatively large owing to the higher requirements for parameter control.

The stimulated Brillouin scattering (SBS) process, as one of the nonlinear effects in optical fibers, has been widely studied and applied in microwave frequency measurement (MFM) [11]–[14]. In Ref. [11], [12], a channelized frequency band based on SBS offers an inherent capability to resolve the problem of mutual constraints between measurement range and accuracy. However, this approach has a more complicated implementation process, which requires two measurement steps, including rough and precise measurements. Besides, the unknown signal frequency can be estimated by introducing the Brillouin frequency shift (BFS) dependence on the optical wavelength [13]. Nevertheless, low-frequency detection is hardly achieved due to the strict requirement of the wavelength tuning process.

In this paper, the frequency of the unknown signal is converted by applying frequency-to-phase-slope mapping (FTPSM). The SBS and optical frequency comb (OFC) pump are combined to realize a channel bandwidth tunable microwave frequency measurement with spectrum-controlled Brillouin phase shift. The linearly arranged multi-tone signals are modulated onto the pump light and combined with the unknown signal. Further, the Brillouin phase shift response that depends on the unknown signal is established to achieve frequency measurement. According to numerical simulation results, it enables flexible frequency measurement in any interested frequency range according to the

Manuscript received September 22, 2021; accepted October 22, 2021. Date of publication October 27, 2021; date of current version November 3, 2021. This work was supported in part by the National Natural Science Foundation of China under Grant 61875070, in part by the Science and technology Development Plan of Jilin Province under Grant 20180201032GX, and in part by the Science and Technology Project of Education Department of Jilin Province under Grant JJKH20190110KJ. *(Corresponding author: Wei Dong.)*

Di Wang, Xindong Zhang, Zhangyi Yang, Cong Du, and Wei Dong are with the State Key Laboratory on Integrated Optoelectronics, College of Electronic Science and Engineering, Jilin University, 130012, China (e-mail: 1913584528@qq.com; xindong@jlu.edu.cn; 1633655100@qq.com; 460545509@qq.com; dongw@jlu.edu.cn).

Shuang Liu is with the Beijing Institute of Radio Metrology and Measurement, Beijing 100039, China (e-mail: 838576471@qq.com).

Jiaqi Li is with the Shanghai Radio Equipment Research Institute, Minhang, Shanghai 201109, China (e-mail: jlu_ljq@163.com).

Digital Object Identifier 10.1109/JPHOT.2021.3123274

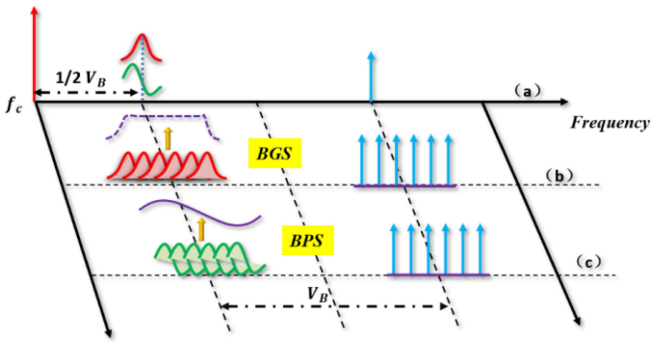

Fig. 1. Conceptual diagram of different response functions. (a) The intrinsic BGS and BPS; (b) The broadened BGS; (c) The broadened BPS.

practical application scenario, which eases the trade-off between frequency range and accuracy. A proof-of-concept experiment is verified with the channel bandwidth of 500, 700, or 900 MHz, and with an error below 35 MHz.

II. Experimental Setup and Principle of Operation

In the SBS process, the Brillouin gain spectrum (BGS) and Brillouin phase spectrum (BPS) are obtained when the frequency difference between the pump light f_p and probe light f_s is close enough to the Brillouin frequency shift V_B of optical fiber [14]. Naturally, the SBS gain and phase shift spectrum are Lorentzian and sinusoidal shape, respectively. Their bandwidth roughly varies from10 to 50 MHz as illustrated in Fig. 1(a), which is mainly related to the characteristics of the fibers [15]. The equations of Brillouin gain and phase shift are given as follows:

$$G_{sbs} = \frac{g_0}{2} \frac{(\Delta v_B/2)^2}{(\Delta v)^2 + (\Delta v_B/2)^2} \tag{1}$$

$$P_{sbs} = \frac{g_0}{4} \frac{\Delta v_B \Delta v}{(\Delta v)^2 + (\Delta v_B/2)^2} \tag{2}$$

where $g_0 = g_B\ I_p L_{eff}/A_{eff}$, g_B is the line center gain coefficient, I_p denotes the power of the pump light, L_{eff} represents effective fiber length, A_{eff} represents effective mode area, Δv_B is Brillouin bandwidth, and Δv is the frequency offset from the center of BGS or BPS [16].

Theoretically, the BGS and BPS responses can be broadened using a pump light consisting of equal-amplitude spectral lines with an interval equal to or less than the SBS bandwidth. The response function $H(\omega)$ can be broadened by convolving the intrinsic BGS of G_{sbs} with the power spectrum of the pump light P_p , which is expressed as [17], [18]:

$$H_G(\omega) \propto G_{sbs} \otimes P_p \tag{3}$$

As illustrated in Fig. 1(b), when the OFC with equal amplitude at each spectral line (blue lines) are the Brillouin pump, the natural BGSs (red curves) are generated and superimposed at one Brillouin frequency shift V_B. A wideband and flat BGS response can be obtained (purple dotted curve). However, a monotonic response with a relatively steep slope is usually required in order to achieve frequency mapping [18]. To solve this problem, a response (purple curve) with a steep slope is generated, which uses the superimposed BPSs (green curves) instead of applying the response constructed through BGSs, as shown in Fig. 1(c). According to Eq. 3, the broadened response of BPSs is shown as follows:

$$H_P(\omega) \propto P_{sbs} \otimes P_p \tag{4}$$

By changing the number of OFC lines, the BPS response has different bandwidths and slopes, which establishes a flexible and reconfigurable frequency measurement system. Meanwhile it further balances the constraints of measurement range and measurement accuracy.

Due to double-sideband suppressed carrier (DSB-SC) modulation in the experiment, two BGS and BPS with the same height are generated after the beat frequency. Further, the second peak is applied to achieve frequency measurement, thus avoiding the frequency ambiguity when it is less than V_B, which has been verified in our previous work [12]. The main process to achieve frequency measurement is as follows: Firstly, fixing the probe signal, a known signal that is close to the frequency of the unknown signal is used to measure the Brillouin phase-shift spectrum, thus obtaining the frequency-to-phase-slope mapping curve before the start of the experiment; During the experiment, the signal to be measured is introduced again as a pump signal, and the measurement results and FTPSM curve are further compared to obtain the frequency of the unknown signal.

The principle of estimating the frequency of unknown signals is shown in Fig. 2. An unknown RF signal, which is applied as an optical carrier and transmitted to the modulator. The electrical spectral lines with an equal frequency interval are modulated and the double-sideband modulation result is achieved, so an unknown RF signal carrying the OFC lines with the equal frequency interval are generated, as depicted in Fig. 2(a). Therefore, the correlation exists between the unknown signal and the optical frequency comb. With the change of the unknown signal from f_0 to f_n in Fig. 2(a), the position of the OFC moves gradually (rectangles filled with different colors), resulting in the change of the phase shift value of the probe light f_s. And $f_s = (f_0 + V_B + 1/2B_w)$ is fixed on the lowest end of the BPS. Since the main lobe of the phase shift spectrum is linear, as shown in Fig. 2(b), a curve in which the unknown signal is proportional to the phase shift value of the fixed probe light f_s is established, and its bandwidth depends on the number of optical frequency combs. Therefore, through the frequency-to-phase-slope mapping, the frequency value of the unknown signal f_x can be finally obtained.

Figure 3 shows the simulation results of inherent BPS and BGS, respectively. It is clear that the shape of BPS and BGS changes as the bandwidth Δv_B increases. But under natural conditions, Δv_B depends on the characteristics of the optical fiber, which is generally a fixed value. Basing on Eq. 3, the Δv_B and g_0 are set to 50 MHz and 5 respectively. In Fig. 4(a), the corresponding broadened BGS is obtained and the spectrum turns out to be a flat response by using multiple pump lights superimposed and a frequency interval of 25 MHz. However, for the superimposed BPSs, a monotonic response with a relatively steep slope is realized, and the simulation result is shown in Fig. 4(b). Meanwhile, by changing the frequency and the number

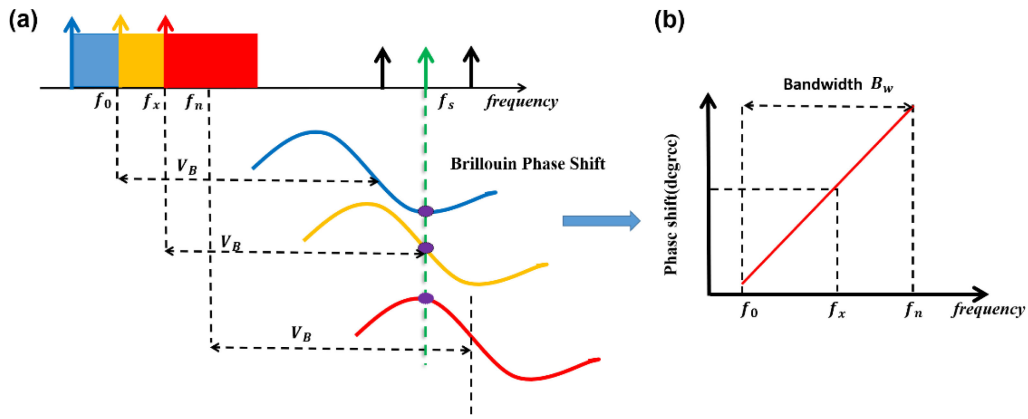

Fig. 2. Principle of estimating the frequency of unknown signals. (a) Schematic diagram of the proposed MFM method; (b) Establish the curve of frequency-to-phase-slope mapping.

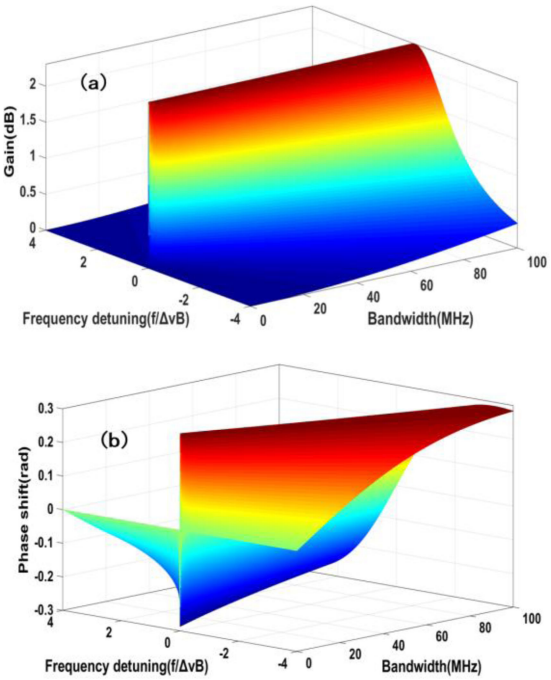

Fig. 3. The simulation results of BGS and BPS respectively.

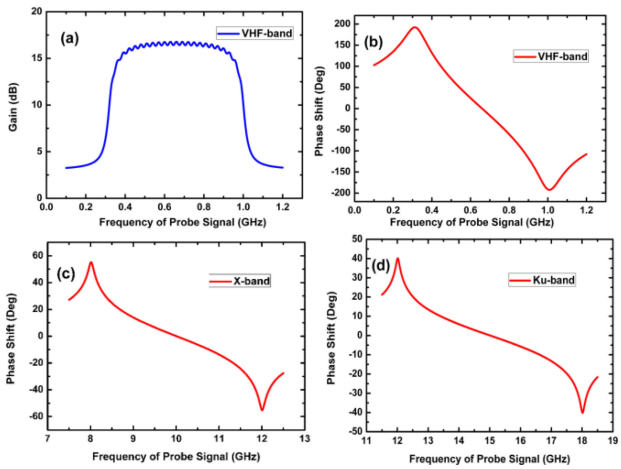

Fig. 4. The simulation results of (a) broadened BGS in VHF-band, (b) broadened BPS in VHF-band, (c) broadened BPS in X-band, (d) broadened BPS in Ku-band.

of comb teeth of OFC pump, arbitrary passband and bandwidth response can be constructed, including VHF-band, X-band, and Ku-band as shown in Fig. 4(b), (c), (d). As shown in Fig. 5, since the information of unknown signal is contained in the pump light, a rising BPS response that changes with the unknown signal is achieved as described in Fig. 2. Instead of using BGS, the broadened BPS response has a relatively steep slope, which further realizes the high-precision frequency measurement through phase-frequency mapping.

In Fig. 5, it can be seen that the monotonic BPS response curve tends to be flat (the y-coordinate, that is, the phase shift range is reduced) as the bandwidth increases, which leads to the decrease of frequency measurement accuracy. This drawback can be remedied by increasing the power of the pump light as shown in Fig. 6. As the power of the pump light gradually increases from 5 mW to 25 mW, the curve becomes steeper within a certain range, further balancing the constraints between the measurement range and the measurement accuracy.

III. Experimental Demonstration

The experimental setup is described in Fig. 7. A continuous wave at f_c emitted from a 1550 nm laser diode is divided into upper and lower branches by a 5:5 coupler. In the upper branch, after a PC, an unknown RF signal f_x from the microwave signal source is launched into MZM1, which is biased at minimum transmission point to realize a DSB-SC modulation. Subsequently, the electrical spectral lines with an equal frequency interval of 25 MHz sent from AWG are modulated to generate the OFC pump lines. With proper bias control of the MZM2, double-sideband (DSB) modulation can be achieved, resulting in a double-effect optical frequency comb. Then, the modulated signals are amplified by an erbium-doped optical fiber amplifier (EDFA1) and transmitted to port 1 of the optical circulator (OC), which enters the single-mode fiber (SMF) as the pump light for the SBS effect. In the lower branch, a series of scanning

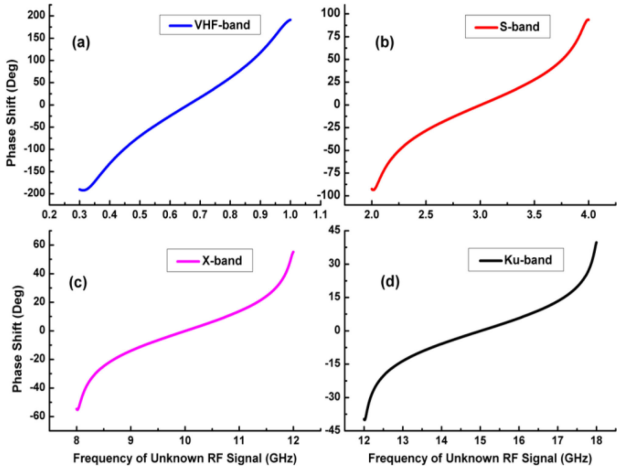

Fig. 5. The curve of frequency-to-phase-slope mapping in different frequency band. (a) VHF-band; (b) S-band; (c) X-band; (d) Ku-band;.

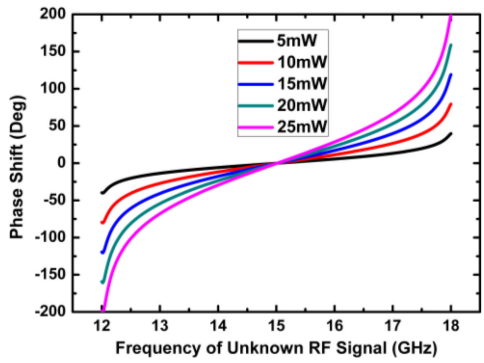

Fig. 6. The BPS response curve changes with pump power value. .

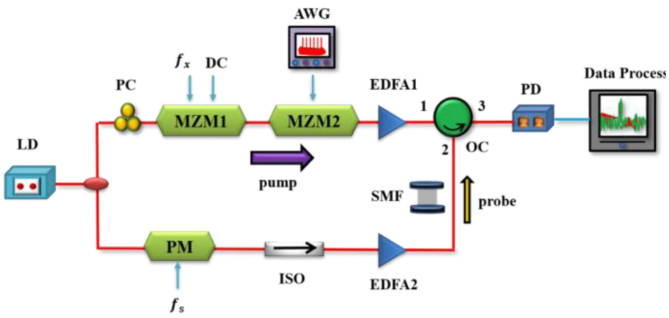

Fig. 7. Experimental setup. LD: laser diode. PC: polarization controller. PM: phase modulator. ISO: isolator. MZM: Mach-Zehnder modulator. EDFA: erbium-doped fiber amplifier. ISO: isolator. OC: optical circulator. SMF: single-mode fiber. PD: photo-detector. AWG: arbitrary waveform generator.

microwave signals f_s generated by the vector network analyzer enters the phase modulator to achieve phase modulation, which is then fed into the optical isolator to ensure unidirectional transmission. Subsequently, the signals are amplified by an EDFA2 and sent to the SMF as probe light. Then, the pump light and probe light with a difference of one BFS are transmitted in SMF, in which the SBS effect occurs. The system response is converted by the photodetector (PD) and displayed in the VNA finally.

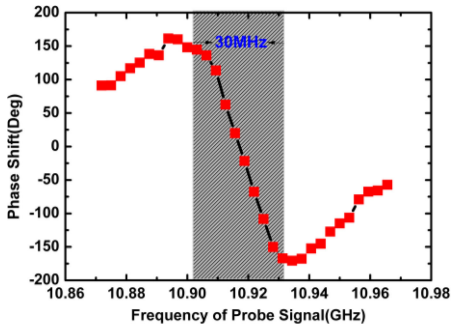

Fig. 8. The inherent BPS response is confirmed by applying a pump light.

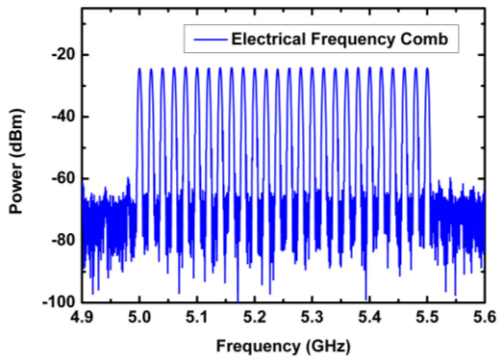

Fig. 9. The electrical frequency comb is generated by the AWG.

Based on Fig. 7 without the AWG, the inherent BPS response is first confirmed by applying a pump light, that is, an unknown signal with a frequency of 0.1 GHz. As shown in Fig. 8, the bandwidth of the available monotone interval in the response of the BPS is 30 MHz, which is covered by the shaded area. Based on this, a broadened BPS response curve will be established by applying the OFC pump. As shown in Fig. 9, instead of controlling the pump spectrum from the time domain, the AWG generates an electrical frequency comb, which guarantees the output spectral lines with equal amplitude and equal intervals of 25 MHz. Restricted by the available modulator, the unknown signal is sent through the AWG together with the electric frequency comb. Then the signal is modulated by the modulator to realize the conversion from electrical to optical, and further used as a Brillouin OFC pump.

When the number of electrical frequency combs are set to 18, with the gradual change of the unknown signal from 13.2 to 13.7 GHz, that is, the change of the OFC pump, the phase shift changes of the fixed probe light of 23.1 GHz are obtained as described in the second part. As a result, the BPS response curve that is broadened to 500 MHz is established with the unknown signal. Therefore, through the frequency-to-phase-slope mapping, the value of the unknown signal is obtained according to the phase shift of the fixed probe light through the fitting curve of Fig. 10(a). Finally, the measurement error within thebandwidth of 500 MHz is obtained in Fig. 10(b), and its maximum measurement error is less than 20 MHz.

In order to prove the flexibility of this method, the BPS response curve of 700 MHz bandwidth ranging from 5.3 to 6 GHz is further confirmed by adjusting the number of OFC

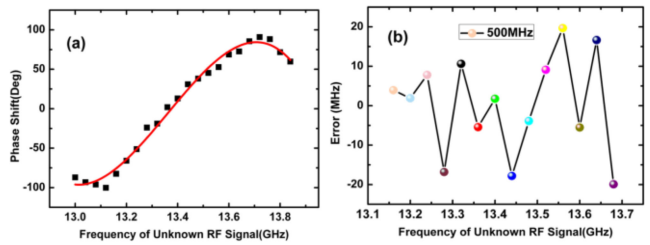

Fig. 10. (a) The BPS response curve that is broadened to 500 MHz with the unknown signal; (b) The measurement error within the bandwidth of 500 MHz.

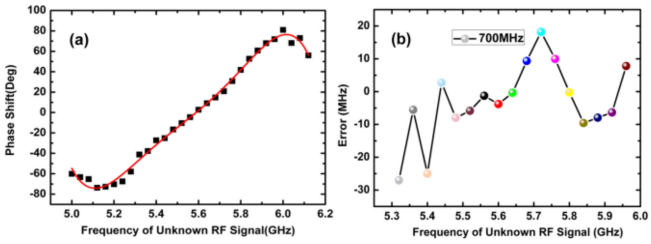

Fig. 11. (a) The BPS response curve that is broadened to 700 MHz with the unknown signal; (b) The measurement error within the bandwidth of 700 MHz.

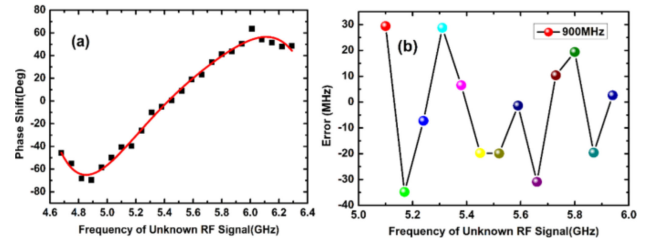

Fig. 12. (a) The BPS response curve that is broadened to 900 MHz with the unknown signal; (b) The measurement error within the bandwidth of 900 MHz.

pump to 26 and changing the frequency of OFC pump. So, with the frequency of probe signal being 15.4 GHz, the obtained frequency-to-phase-slope mapping is shown in the Fig. 11(a), and the fitting curve is shown in the red line. It can be seen from Fig. 11(b) that the maximum measurement error is less than 30 MHz.

Meanwhile, from Fig. 12(a) and (b), the experimental results that the bandwidth of BPS response curve is 900 MHz at 5.1 GHz and the maximum measurement error is less than 35 MHz are also realized. For comparison, the intrinsic SBS phase spectrum is shown in Fig. 8 and the bandwidth is only 30 MHz, where no OFC pump and no spectrum shaping are implemented. Therefore, an adjustable channel bandwidth of 500, 700 MHz, or 900 MHz, which is of greatly importance for the microwave measurement, is realized via the spectrum-controlled SBS effect.

IV. Conclusion

In summary, we have theoretically and experimentally demonstrated the photonic MFM with the channel bandwidth of 500, 700, or 900 MHz, with an error of 35 MHz. A spectrum-controlled Brillouin phase shift curve is constructed to realize the frequency-to-phase-slope mapping, further enabling the frequency measurement. The proposed method adjusts the response bandwidth by simply controlling the number of optical frequency combs, thereby achieving a flexible frequency measurement range. Compared with the frequency-to-power/time mapping method, it avoids the high requirements and precise control for devices, such as the optical filtering shape and the optical carrier wavelength. More importantly, it enables flexible frequency measurement in any interested frequency range, such as C-band, X-band, and Ku band, and it also has the potential to be developed in radio frequency channelized receiver according to demand and guarantee accuracy.

References

[1] J. B. Y. Tsui, *Digital techniques for wideband receivers*, 2nd ed. Raleigh, NC, USA: SciTech, 2004.

[2] X. Zou, W. Li, W. Pan, L. Yan, and J. Yao, "Photonic-assisted microwave channelizer with improved channel characteristics based on spectrum-controlled stimulated Brillouin scattering," *IEEE Trans. Microw. Theory Techn.*, vol. 61, no. 9, pp. 3470–3478, Sep. 2013.

[3] Y. Shao, X. Han, M. Li, Q. Liu, and M. Zhao, "Microwave down-conversion by a tunable optoelectronic oscillator based on PS-FBG and polarization multiplexed dual-loop," *IEEE Trans. Microw. Theory Tech.*, vol. 67, no. 5, pp. 2095–2102, May 2019.

[4] X. Zou and J. Yao, "An optical approach to microwave frequency measurement with adjustable measurement range and resolution," *IEEE Photon. Technol. Lett.*, vol. 20, no. 23, pp. 1989–1991, Dec. 2008.

[5] Y. Li, "Instantaneous microwave frequency measurement with improved resolution," *Opt. Commun.*, vol. 354, pp. 140–147, 2015.

[6] H. Wang, S. J. Zhang, X. H. Zou, Z. Y. Zhang, Y. L. Zhang, and Y. Liu, "Photonic microwave frequency measurement based on frequency-configurable pilot tones," *IEEE Photon. Technol. Lett.*, vol. 30, no. 4, pp. 363–366, Feb. 2018.

[7] J. Zhou, S. Fu, S. Aditya, P. P. Shum, and C. Lin, "Instantaneous microwave frequency measurement using photonic technique," *IEEE Photon. Technol. Lett.*, vol. 21, no. 15, pp. 1069–1071, Aug. 2009.

[8] X. Li, "Photonic microwave frequency measurement with a tunable range based on a dual-polarization modulator," *Appl. Opt.*, vol. 55, pp. 8727–8731, 2016.

[9] T. A. Nguyen, E. H. W. Chan, and R. A. Minasian, "Instantaneous high-resolution multiple-frequency measurement system based on frequency-to-time mapping technique," *Opt. Lett.*, vol. 39, no. 8, pp. 2419–2422, 2014.

[10] H. Emami, M. Hajihashemi, S. E. Alavi, A. S. M. Supaat, and L. Bui, "Microwave photonics instantaneous frequency measurement receiver based on a Sagnac loop," *Opt. Lett.*, vol. 43, no. 10, pp. 2233–2236, 2018.

[11] H. Jiang *et al.*, "Wide-range, high precision multiple microwave frequency measurement using a chip-based photonic Brillouin filter," *Optica*, vol. 3, no. 1, pp. 30–34, 2016.

[12] D. Wang, L. Pan, and Y. Wang, "Instantaneous microwave frequency measurement with high-resolution based on stimulated Brillouin scattering," *Opt. Laser Technol.*, vol. 113, pp. 171–176, 2019.

[13] S. Shakthi, A. Suresh, V. Reddy, and R. Pant, "Wideband instantaneous frequency measurement using stimulated Brillouin scattering," in *Proc. Photon. Fiber Technol. Congr.*, 2016, pp. AT5C-5.

[14] X. Long, W. Zou, and J. Chen, "Broadband instantaneous frequency measurement based on stimulated Brillouin scattering," *Opt. Exp.*, vol. 25, no. 3, pp. 2206–2214, 2017.

[15] W. Wei, L. L. Yi, Y. Jaouën, and W. S. Hu, "Bandwidth-tunable narrowband rectangular optical filter based on stimulated Brillouin scattering in optical fiber," *Opt. Exp.*, vol. 22, no. 19, pp. 23249–23260, 2014.

[16] C. Du, X. Li, and D. Wang, "Photonic generation of MMW-UWB monocycle and doublet signals based on frequency up-conversion and delay-line filter," *Opt. Commun.*, vol. 445, pp. 241–246, 2019.

[17] Q. Zhang, J. Zhang, and Q. Li, "Bandwidth tunable microwave photonic filter based on digital and analog modulation," *Opt. Fiber Technol.*, vol. 42, no. 3, pp. 34–38, 2018.

[18] W. Zou, X. Long, X. Li, G. Xin, and J. Chen, "Brillouin instantaneous frequency measurement with an arbitrary response for potential real-time implementation," *Opt. Lett.*, vol. 44, no. 8, pp. 2045–2048, 2019.